Models for Oxygenases That Catalyze the Cleavage of Carbon–Carbon Bonds: Kinetics and Mechanism of the Decomposition of 2,3-Dimethyl-3-peroxyindolenines in Aqueous Solution[1]

Mark S. Fraser and Gordon A. Hamilton*

Contribution from the Department of Chemistry, The Pennsylvania State University, University Park, Pennsylvania 16802. *Received June 5, 1981*

Abstract: At 41 °C in aqueous solution, 2,3-dimethyl-2-(hydroperoxy)indolenine (**6**) and 2,3-dimethyl-3-(methylperoxy)indolenine (**7**) react according to first-order kinetics to give, depending on pH, *o*-acetamidoacetophenone (**8**), 2,3-butanedione (biacetyl), or a mixture of the two in virtually quantitative yield. The pH–rate and product profiles obtained with **6** and **7** show some similarities but are not identical. With **7** as reactant the rate constant for formation of each product is characterized by a bell-shaped curve, the half-maximum points being at ca. pH 2.2 and 6 for biacetyl formation and at 6 and 7.5 for the formation of **8**. Compound **6** reacts more rapidly and over a broader pH range; the overall first-order rate constant is at a maximum and relatively constant from pH 4 to 10, but it decreases at low and high pH. Above pH 7, **8** is the only product, but a mixture of **8** and biacetyl are formed at lower pHs. The pK_as of protonated **6** and **7** were found to be 2.28 and 2.18, respectively. Studies with ^{18}O-labeled **6** indicate that at pH 4 **8** is formed with essentially 100% of the amide group labeled, but at higher pHs, the amount of unlabeled oxygen in this position increases to a maximum of 50% at pHs 9 to 12.6. The results with **7** can be quantitatively rationalized in terms of a mechanism that involves cis and trans isomers of a carbinolamine (formed by hydration of **7**) as important intermediates. Both geometric isomers can give biacetyl through a ring-opened intermediate that undergoes a carbon to oxygen migration of the aryl group. Only one geometric isomer can give **8**, apparently by rapid decomposition of the alkoxide formed from the intermediate carbinolamine. The reaction of **6** is too complex to be able to fit the data quantitatively to a particular reaction mechanism, but qualitative considerations indicate that **8** can be formed from **6** by three different mechanisms that all seem to be competing under the reaction conditions. The relevance of these findings to related enzymic reactions is briefly considered.

It is now evident that a number of oxygenases catalyze the carbon–carbon bond cleavage of compounds such as **1** or **2** to give carbonyl products **3** and **4** (or a dicarbonyl product if the bond cleaved is part of a ring). Various such oxygenases are involved in the cleavage of phenols and indoles,[2] in bioluminescent reactions,[3] and in the conversion of ribulose bisphosphate to phosphoglycolate and 3-phosphoglycerate.[4] Essentially all reasonable mechanisms for these reactions have as a first step the formation of an α-hydroperoxy ketone or imine (**5**), most likely by some free radical or metal ion assisted mechanism.[5] However, there are several possible pathways by which **5** can react to give **3** and **4**, and three that have received considerable discussion in the literature[2-14] are outlined in eq 1. Pathway a, the so-called "linear" mechanism, involves initial hydration followed by dehydration as shown, pathway b has a dioxetane intermediate, and pathway c involves an initial rearrangement (the mechanistic arrows associated with **5** are for this pathway) equivalent to the *trans*-decalyl

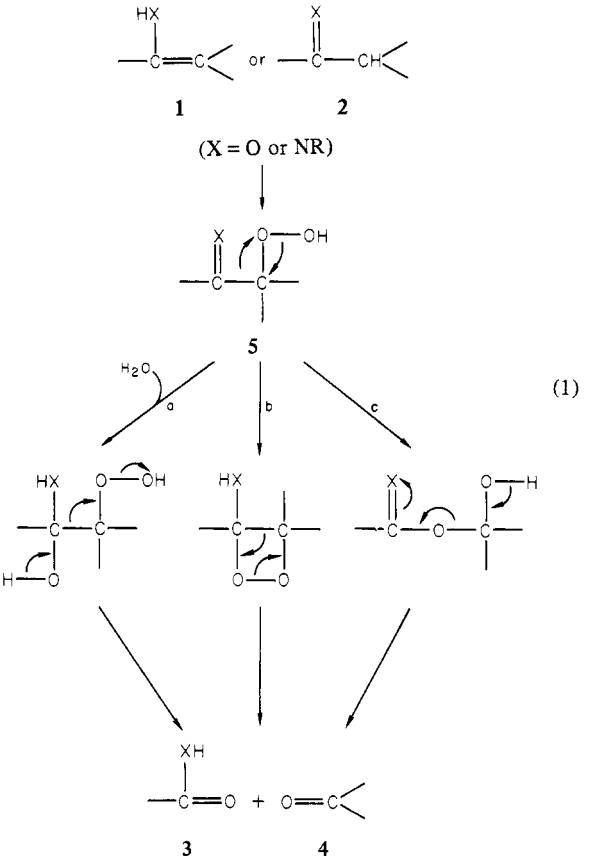

(1)

(1) This research was supported by a grant (AM 13448) from the National Institute of Arthritis, Metabolism and Digestive Diseases, Public Health Service.

(2) (a) Nozaki, M. In "Molecular Mechanisms of Oxygen Activation"; Hayaishi, O., Ed; Academic Press: New York, 1974; pp 135–165. (b) Feigelson, P.; Brady, F. O. *Ibid.*; pp 87–133. (c) Hayaishi, O.; Nozaki, M.; Abbott, M. T. *Enzymes, 3rd Ed.* **1975**, *12*, 120–189. (d) Nozaki, M. *Top. Curr. Chem.* **1979**, *78*, 145–186.

(3) (a) Hart, R. C.; Cormier, M. J. *Photochem. Photobiol.* **1979**, *29*, 209–215. (b) Hastings, J. W.; Wilson, T. *Ibid.* **1976**, *23*, 461–473.

(4) (a) Pierce, J.; Tolbert, N. E.; Barker, R. *J. Biol. Chem.* **1980**, *255*, 509–511. (b) McFadden, B. A. *Acc. Chem. Res.* **1980**, *13*, 394–399.

(5) (a) Hamilton, G. A. *Adv. Enzymol.* **1969**, *32*, 55–96. (b) Hamilton, G. A. In "Molecular Mechanisms of Oxygen Activation"; Hayaishi, O., Ed; Academic Press: New York, 1974; pp 405–451.

(6) (a) Saito, I.; Matsuura, T.; Nakagawa, M.; Hino, T. *Acc. Chem. Res.* **1977**, *10*, 346–352. (b) Matsuura, T. *Tetrahedron* **1977**, *33*, 2869–2905. (c) Saito, I.; Matsugo, S.; Matsuura, T. *J. Am. Chem. Soc.* **1979**, *101*, 4757–4759, 7332–7338. (d) Nakagawa, M.; Kato, S.; Kataoka, S.; Hino, T. *Ibid.* **1979**, *101*, 3136–3137. (e) Nakagawa, M.; Watanabe, H.; Kodata, S.; Okajima, H.; Hino, T.; Flippen, J. L.; Witkop, B. *Proc. Natl. Acad. Sci. U.S.A.* **1977**, *74*, 4730–4734.

(7) Richardson, W. H.; Hodge, V. F.; Stigall, D. L.; Yelvington, M. B.; Montgomery, F. C. *J. Am. Chem. Soc.* **1974**, *96*, 6652–6657.

(8) Sawaki, Y.; Ogata, Y. *J. Am. Chem. Soc.* **1975**, *97*, 6983–6989; **1977**, *99*, 5412–5416.

(9) Sawaki, Y.; Foote, C. S. *J. Am. Chem. Soc.* **1979**, *101*, 6692–6296.

(10) Jefford, C. W.; Knöpfel, W.; Cadby, P. A. *J. Am. Chem. Soc.* **1978**, *100*, 6432–6436.

(11) Muto, S.; Bruice, T. C. *J. Am. Chem. Soc.* **1980**, *102*, 7379–7381.

(12) Que, L., Jr.; Lipscomb, J. D.; Munck, E.; Wood, J. M. *Biochim. Biophys. Acta* **1977**, *485*, 60–74.

(13) Saeki, Y.; Nozaki, M.; Senoh, S. *J. Biol. Chem.* **1980**, *225*, 8465–8471.

(14) May, S. W.; Phillips, R. S. *Biochemistry* **1979**, *18*, 5933–5939.

0002-7863/82/1504-4203$01.25/0

perester rearrangement first described by Criegee.[5] By utilizing isotopically labeled O_2, it is easy to distinguish a reaction that proceeds by pathway a from one that goes by either of the other pathways of eq 1, and for this reason it is generally considered that ribulosebisphosphate oxygenase catalyzes its reaction by pathway a while the arene cleavage dioxygenases and the bioluminescent reactions[15] proceed by either b or c.

Because the isotopic data alone cannot distinguish between reactions that proceed by b or c, other approaches must be employed. There is abundant evidence in the literature that both pathways b and c do occur in various nonenzymic systems,[6,10,11,16] but most of the information available is based on product identification and was obtained from reactions run in organic solvents or under strongly basic conditions. Since the enzymic reactions occur at neutral pH in aqueous solution, it was felt that a detailed kinetic and product study of a reaction that proceeds under such conditions might give further information concerning which pathway is more likely, what conditions favor a particular pathway, and how an enzyme might catalyze reactions by each pathway. Because we were interested in characterizing the steps from the intermediate peroxide **5** to the products, we felt it important to choose a system where **5** could be isolated in pure form so that there would be no complexities caused by the requirement to produce the intermediate from **1** or **2** in the reaction mixture. For these and other reasons, we chose to study in detail the reactions of 2,3-dimethyl-3-(hydroperoxy)indolenine (**6**) and 2,3-dimethyl-3-(methylperoxy)indolenine (**7**). Compound **6** is a specific

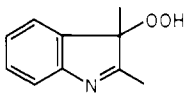

6

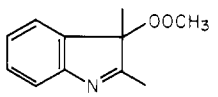

7

compound that has the structural features of **5**, and its methyl derivative **7** was studied to see how the reaction changed when pathway b was eliminated as a possibility. The reactions of **7** turned out to be considerably easier to analyze than those of **6**, so for this reason the detailed results obtained with **7** are presented and discussed first. Following the discussion of the results obtained with **6**, some brief comments concerning the relevance of the findings to enzymic reactions are made. It will become evident that the rearrangement pathway given in eq 1 is somewhat oversimplified but that the alternate rearrangement mechanism can also explain all the data now available on the enzymic reactions thought to proceed by either pathway b or c.

Results

General Characteristics of the Reactions of 6 and 7. At ca. 40 °C and neutral pH, both **6** and **7** react to give products at a rate that is conveniently measured (half-times of minutes to hours). At pHs above 7.5 with either **6** or **7** as reactant, *o*-acetamidoacetophenone (**8**) is formed in virtually quantitative yield[17] as indicated by its UV spectrum and analysis by gas chromatography. However, at lower pHs the yield of **8** drops, and other products are formed. One of these is 2,3-butanedione (biacetyl), which was positively identified both by its retention time on gas chromatography (GC) and by its identity with authentic biacetyl when subjected to gas chromatography–mass spectrometry (GC–MS). When biacetyl is formed, one suspects that *o*-aminophenol should also be present in stoichiometric quantities. However, due to the instability of this compound under the reaction conditions, it was not possible to analyze quantitatively for it. Nevertheless, at low pHs the UV spectra of completed reaction solutions indicate the presence of a peak at ca. 270 nm, which is where *o*-aminophenol absorbs. Furthermore, if these solutions are allowed to autoxidize over a period of days, the spectra observed are very similar to those seen when authentic *o*-aminophenol is subjected to the same conditions. Biacetyl and **8** are stable to the reaction conditions from pH 0 to 12, and their total yield is always greater than 80% and usually greater than 90%. Thus, in this pH region all the reactions that are occurring can presumably be summarized as shown in eq 2. No analysis for methanol was attempted, but one suspects it is also formed when the reactant is **7**.

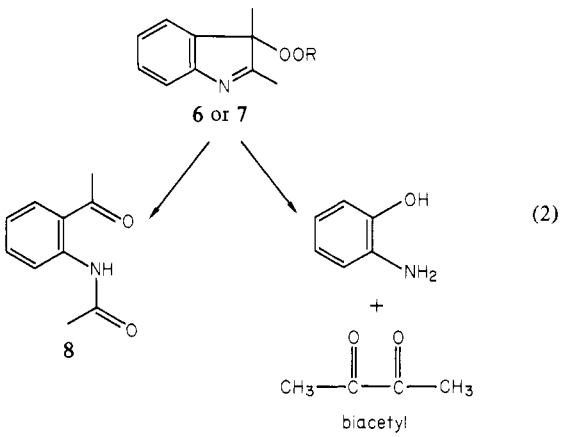

(2)

When measured by the change in absorbance (a decrease at 280 nm for reactions at pHs less than 5 and an increase at 325 nm for reactions at pHs above 5) with time, it was found over the pH range studied that **6** and **7** react according to first-order kinetics. Such plots of the absorbance data are linear for 3–4 half-lives of the reaction in carefully monitored runs and for at least 2 half-lives in routine runs. Variation in the initial concentration of **6** or **7** from about 0.15 to 1.0 mM has no effect on k_{obsd}, the observed first-order rate constant. Over the course of this work, various preparations of **6** and **7** were used, and there was no detectable change in k_{obsd} from one preparation to another or over a period of time with the same preparation. In other experiments it was found that molecular oxygen has no effect on the reaction; experiments performed in the presence or absence of O_2 proceed at the same rate and yield the same mixture of products. Although EDTA (0.1 mM) was used throughout in order to prevent possible complications caused by small amounts of trace metal ions, no effect of EDTA was noted in control experiments. Ionic strength has only a small effect on the observed first-order rate constant; at pH 7.0 with **6** as reactant, a 5-fold increase in μ (from 0.1 to 0.5) causes an increase in the rate constant of only 25%. Nevertheless, for most of the kinetic experiments reported, the ionic strength was kept constant at 0.3 (by using KCl in addition to the buffer). Neither the identity of the buffer nor its concentration over the range of concentrations investigated (0.01–0.1 M) was found to have any detectable effect on k_{obsd} or on the relative yield of products. This was checked at each pH for which kinetic and product data were collected. Changing the solvent from H_2O to D_2O has only a small effect on the rate at neutral pH. Thus with **6** as reactant at 40 °C in 0.01 M phosphate buffer, pH 7.0 (in H_2O; in D_2O the same ratio of acid and base components was used that give pH 7.0 in H_2O), $k_{H_2O}/k_{D_2O} = 1.24$, and in both solvents the yield of **8** is greater than 85%.

Effects of pH on the Reaction of 7. Given in Figure 1 are some data illustrating these effects. The points given in the figure are the experimental results whereas the lines are theoretical ones based on a particular mechanism and derived rate constants as discussed in the next section. The circles are the observed first-order rate constants (k_{obsd}) calculated from the absorbance changes with time, while the squares and triangles represent the rate constants for formation of **8** and biacetyl, respectively, from pH 5.5 to 7.0, the region in which both products are formed in significant amounts. Below pH 5, biacetyl is essentially the only product, and above pH 7.5, **8** is the exclusive product. The rate constants for formation of the products were obtained by mul-

(15) Despite the fact that various authors interested in bioluminescent reactions[3] assume that the isotopic results indicate pathway b is operative in these systems, all the evidence is equally consistent with their proceeding by a rearrangement mechanism.

(16) George, M. V.; Bhat, V. *Chem. Rev.* **1979**, *79*, 447–478.

(17) At pHs greater than 12, **8** begins to hydrolyze under the reaction conditions to *o*-aminoacetophenone and presumably acetate (at pH 12.6, ca. 35% of **8** is hydrolyzed after 6 h at 41 °C), but up to pH 12.6 the total yield of **8** and *o*-aminoacetophenone still remains greater than 80%.

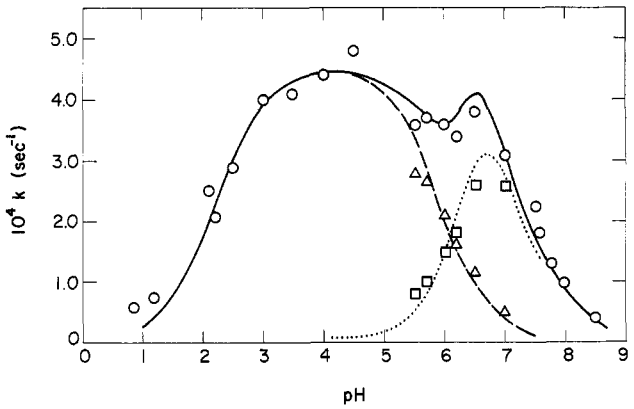

Figure 1. Dependence of the first-order rate constants on pH for the reaction of **7** at 41 °C: (○) rate constant for the overall reaction (k_{obsd}) obtained from spectral measurements; (□) rate constant (k_{amide}) for the formation of **8** from pH 5.5 to 7.0; (△) rate constant (k_{biac}) for the formation of biacetyl from pH 5.5 to 7.0. The buffers used are the following: HCl from pH 0.8 to 2.2, chloroacetate from pH 2.1 to 3.0, succinate from pH 3.5 to 6.0, phosphate from pH 6.0 to 7.5, and Tris·HCl from pH 7.0 to 8.5. The lines represent theoretical curves (k_{obsd}, solid line; k_{amide}, dotted line; and k_{biac}, dashed line) calculated for a particular mechanism as described in the text.

tiplying k_{obsd} by the mole fraction of that particular product observed at the end of the reaction. Thus, the rate constant for formation of the amide **8** is given by eq 3 and that for the for-

$$k_{amide} = k_{obsd}[\mathbf{8}]/([\mathbf{8}] + [\text{biacetyl}]) \quad (3)$$

mation of biacetyl is given by eq 4. Since the products are

$$k_{biac} = k_{obsd}[\text{biacetyl}]/([\mathbf{8}] + [\text{biacetyl}]) \quad (4)$$

obtained in virtually a quantitative yield and since both are formed according to first-order kinetics, this treatment of the data is valid. Kinetic results obtained between pH 4.5 and 5.5 are not given in the figure because the rate constants obtained were not reproducible due to the small absorbance changes that occurred during the reaction in this pH region. As determined by the spectral method described in the Experimental Section, the pK_a of protonated **7** was found to be 2.18 ± 0.03.

Effects of pH on the Reaction of 6. The observed first-order rate constants (k_{obsd}), determined by UV spectroscopy at various pHs, are not only given in Table I but are also plotted in Figure 2 (open circles). It can be seen that the overall rate constant for reaction of **6** is at a maximum and relatively constant from pH 4 to 10, but it decreases at low and high pH. The decrease at high pH probably is due to the ionization of the hydroperoxy group whose pK is expected to be ca. 11. However, the decrease below pH 4 cannot be correlated with any single ionization; it must be due to more than one change in either a rate-determining step or the ionization of some intermediate. Even at pHs between 4 and 10, there may be small changes in the rate constant since several of the points seem outside the reproducibility (±5%) of individual runs. No significance should be attached to the lines drawn through the points of Figure 2 because these are just qualitative approximate fits to the experimental data.

Using eq 3 and 4 and the product yields obtained as a function of pH (Table I), one can calculate the first-order rate constants for the formation of **8** and biacetyl, and these are also plotted in Figure 2. It is evident from such plots, as well as from the data in Table I, that biacetyl is the exclusive product at low pHs (below 1) while the amide is the only product formed at pHs above 7. The initial increase in k_{amide} as the pH is raised correlates well with the pK_a of protonated **6**, which was independently determined to be 2.28 ± 0.03. The subsequent increase in k_{amide} at higher pHs (5–6.5) occurs in a pH range where k_{biac} is decreasing, and both occur in a region where **6** does not ionize.

Studies with ^{18}O-Labeled 6 and 7. Some preliminary experiments were performed to show that the ^{18}O content of the two oxygens of **8** could be measured separately. When unlabeled **8** is dissolved in $H_2{}^{18}O$ and allowed to remain at 40 °C for 2 h, some ^{18}O is incorporated. With this material, it was found that the ratio of the intensity of the peak at m/z 137 to that at 135 ($I_{137/135}$) is essentially the same as the $I_{179/177}$ ratio, i.e., the ratio of in-

Table I. Rate Constants and Product Yields as a Function of pH for the Reaction of **6** in Aqueous Solution[a]

pH[b]	buffer[c]	k_{obsd},[d] $\times 10^4$ s^{-1}	% yield[e]	
			2	biacetyl
0.4[f]	HCl	3.5	2	81
0.7	HCl	4.1	2	102
1.2	HCl	4.7	6	99
1.6	HCl	5.1	14	84
2.0	CA	6.2	23	74
2.2	HCl	6.9	26	59
2.5	CA	7.8	40	62
3.0	CA, S	7.6	52	43
3.5	S	8.7	54	38
4.0	S	9.3	53	42
4.5	S	9.8	54	
5.0	S	9.3	58	32
5.5	S	9.4		
6.0	S, P	9.3	76	11
6.5	P	10.3		
7.0	P	9.8	88	2
7.5	P	9.4	80	
8.0	P, T	9.2	87	
8.5	T	8.8	84	
9.0	T, C	9.0	98	
9.5	C	8.9	96	
10.0	C	9.4	98	
10.5	C	8.4	92	
11.0	C, P	6.8	90	
11.5	P	5.1	94	
11.9	NaOH	3.8	95	
12.2	NaOH	3.2	88	
12.6	NaOH	2.9	85[g]	

[a] General reaction conditions: temperature, 41.0 °C; buffer concentration = 0.01–0.1 M; μ = 0.30; [**6**] = 0.1–0.2 mM initially; [EDTA] = 0.1 mM; solvent composition, 99.4% H_2O, 0.6% *tert*-butyl alcohol. [b] Recorded at 40 °C. [c] Code: CA, chloroacetate; S, succinate; P, phosphate; T, Tris·HCl; C, carbonate. [d] Values reported are averages of multiple runs (usually 3–6) at various buffer concentrations (from 0.01 to 0.1 M) and are reproducible to ±5% of their values. [e] Reported values are averages of multiple analyses (usually 2–4) and were generally reproducible to ±5% of their values. [f] μ = 1.0. [g] Total yield of **8** and *o*-aminoacetophenone.

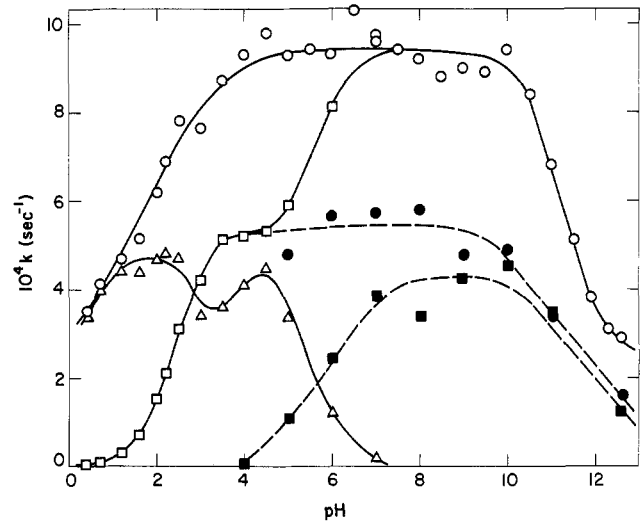

Figure 2. First-order rate constants for the overall reaction of **6** and for the formation of various products from **6** as a function of pH. Experimental conditions are given in the footnotes to Table I and II: (–○–) k_{obsd}; (–△–) k_{biac}; (–□–) k_{amide} at pH 7 and below (above pH 7, k_{amide} = k_{obsd}); (- -●- -) $k_{^{18}O\text{-amide}}$ at pHs above 4 (below pH 4, k_{amide} = $k_{^{18}O\text{-amide}}$); and (- -■- -) $k_{^{16}O\text{-amide}}$. For definitions of the various terms, see the text.

Table II. Oxygen-18 Content of the Oxygens of 8 on Reaction of 6-^{18}O in $H_2{}^{16}O$[a]

	% labeled with ^{18}O[b]	
pH	ketone oxygen	amide oxygen
4	74	101
5	91	81
6	86	70
7	49	60
8	14	63
9	2	53
10	2	52
11	2	49
12.6	2	55[c]

[a] Reaction conditions were the same as given in footnote *a* of Table I. [b] Results are averages of 2-4 runs at pHs of 4-8 (reproducible to ±10% of their values) and are single results at other pHs. [c] Extrapolated to time zero[21] in order to take into account the observation that 8 exchanges its amide oxygen under these conditions.

tensities of the parent ions. Thus, in the fragmentation of the parent ion to the 135 and 137 ions, no loss of ^{18}O label occurs. Since the conversion of an ion at m/z 177 to one at m/z 135 involves the loss of C_2H_2O, these results indicate that **8** has only one readily exchangeable oxygen, and this oxygen is present in the 135 fragment. In another experiment, **8**-^{18}O was prepared by reaction of **6**-^{18}O at pH 7.0, and it was found that both the $I_{179/177}$ and $I_{137/135}$ ratios indicate the presence of ^{18}O, but the former ratio is considerably greater. In a typical case, $I_{179/177}$ = 0.255 and $I_{137/135}$ = 0.135. After this sample of **8**-^{18}O was boiled for 2 h in $H_2{}^{16}O$ (pH 7.0), the $I_{179/177}$ ratio dropped some to 0.137, but the $I_{137/135}$ dropped to 0.010, which is essentially that expected from natural abundance levels of isotopes. However, the difference between the $I_{179/177}$ and the $I_{137/135}$ ratios remains constant, indicating that a nonexchangeable oxygen is lost on fragmentation of the ion at m/z 177 to one at m/z 135. These results are consistent with repeated observations that ketones are readily exchangeable under these conditions while amides are not[18] and that acetanilides readily fragment a ketene moiety in the mass spectrometer.[19,20] Furthermore, they conclusively show that the $I_{137/135}$ ratio is a direct measure of the ^{18}O content of the ketone oxygen, and since the $I_{179/177}$ ratio includes both the ketone and amide oxygens, the ^{18}O content of the amide oxygen can be determined by difference, as outlined in the Experimental Section.

Given in Table II are some data showing the effect of pH on the extent of labeling of the ketone and amide oxygens of **8** when **6**-^{18}O is reacted in $H_2{}^{16}O$. Almost any mechanism for the **6** to **8** conversion predicts that the ketone oxygen should remain 100% labeled, and that is closely approximated at pH 5–6. The decrease in the amount of label observed in this position at lower and higher pHs is almost certainly due to subsequent exchange[18] of the ketone oxygen after the **6** to **8** conversion has occurred. Of more mechanistic interest is the extent of labeling of the amide oxygen. It will be seen that at pH 4, this oxygen is derived completely from one of the peroxide oxygens of **6**, but as the pH is increased, there is a gradual increase in the amount of solvent oxygen that gets incorporated into this position. At pHs 9 and above essentially 50% of the amide oxygen comes from **6** and 50% from the solvent. Since there is no detectable exchange of the amide oxygen of **8** with solvent under the reaction conditions for all pHs from 4 to 12, the incorporation of solvent oxygen must occur during the conversion of **6** to **8**. At pH 12.6, a slow exchange of the amide oxygen of **8** with solvent does occur, so the value reported in Table II for this pH was obtained after extrapolation to zero time.[21] Using the data of Tables I and II, one can calculate first-order rate constants for the formation of ^{18}O amide ($k_{^{18}O\text{-amide}}$) and ^{16}O amide ($k_{^{16}O\text{-amide}}$) by multiplying k_{amide} by the fraction of the product that contains each of the isotopes. These values are plotted in Figure 2 (closed symbols). The dashed lines drawn through these points are again only approximate fits to the data; it seems very likely that the curves are more complex than indicated since several of the points seem to deviate from these simple lines by more than the expected experimental error.

Table III. Effects of Buffer Concentration and of D_2O on the Extent of Labeling of 8 Formed from 6-^{18}O[a]

			% labeled with ^{18}O	
solvent	pH	buffer concn,[b] M	ketone oxygen	amide oxygen
H_2O	7.0	0.20	44	55
H_2O	7.0	0.10	50	68
H_2O	7.0	0.01	52	64
D_2O	(7.0)[c]	0.01	61	71
H_2O	8.0	0.20	9	63
H_2O	8.0	0.10	10	67
H_2O	8.0	0.01	11	68
H_2O	7.8	0.01		64
D_2O	(7.8)[c]	0.01		65
H_2O	9.0	0.10	2	52
H_2O	9.0	0.05	1	56
H_2O	9.0	0.01	2	60
D_2O	(9.0)[c]	0.01	10	51

[a] Reaction conditions were the same as given in footnote *a* of Table I except that μ = 0.6. [b] Phosphate buffers used at pHs 7, 7.8, and 8, and carbonate used at pH 9. [c] Not measured; the ratios of the concentrations of the acid to base forms of the buffer were constant from H_2O to D_2O at the pH value of the H_2O buffers.

Some experiments were performed to determine whether the concentration of the buffer or changing the solvent from H_2O to D_2O had any effect on the amount of label that ends up in the amide oxygen when **6**-^{18}O is reacted in ^{16}O solvents. These results are summarized in Table III. It will be seen that within experimental error there is no effect of these variables from pH 7 to 9.

When **7** labeled with ^{18}O in the peroxide oxygens is allowed to react at pH 7–8, only 4–5% of the product has an ^{18}O label in the amide carbonyl of **8**. Since the sample of **7**-^{18}O used for these reactions had a small amount of **8** as an impurity, it is felt that most, if not all, of the label in this position arose from the impurity formed during the preparation of **7**-^{18}O. Thus, during the reaction of **7**, essentially all of the oxygen in the amide carbonyl of **8** must come from the solvent.

Effects of Added Amines on the Reaction of 6. Since the foregoing studies with **6**-^{18}O indicate that the solvent is participating in the conversion of **6** to **8**, the effects of added nucleophiles (especially amines) on the reaction were investigated. From pH 8 to 10, it was found that various amines (such as hydroxylamine, diethylamine, and morpholine) at concentrations from 0.02 to 0.5 M increased the rate of reaction of **6** by up to 3- or 4-fold and concomitantly led to a decrease in the yield of **8**. A TLC and UV analysis of the products formed under such conditions indicated the presence of a new product, which appears to be 2,3-dimethyl-3-hydroxyindolenine. Since the formation of this product indicates that these nucleophiles are reacting in an entirely different way (presumably the amine is just getting oxidized to the amine oxide) than in the usual **6** to **8** conversion, these reactions were not investigated further.

Reactions of 6 in Ethanol. Again because H_2O appears to be participating directly in the **6** to **8** conversion in aqueous solutions, some experiments were performed in ethanol to determine how the reaction changed when a different hydroxylic solvent was employed. In absolute ethanol and even in ethanol containing 10% water, **6** reacts very slowly at a rate which is only approximately 1–2% of the rate in water at pH 7. With 0.05–0.1 M sodium ethoxide present in absolute ethanol, **6** reacts at 41 °C with a rate constant of 2×10^{-3} s^{-1} to give a greater than 80% yield of **8**. This is approximately 8-fold faster than the reaction of **6** in aqueous solution when it is fully ionized (pH 12.6). Reaction of **6**-^{18}O in 0.1 M ethanolic ethoxide gives **8** that has ca. 90% ^{18}O in the amide oxygen.

(18) Samuel, D.; Silver, B. L. *Adv. Phys. Org. Chem.* **1965**, *3*, 123–186.
(19) Benezra, S. A.; Bursey, M. M. *J. Chem. Soc. B* **1971**, 1515–1520.
(20) Burcharts, D. *Acta Chem. Scand.* **1968**, *22*, 2329–2337.
(21) Fraser, M. S. Ph.D. Thesis, The Pennsylvania State University, 1977.

Scheme I

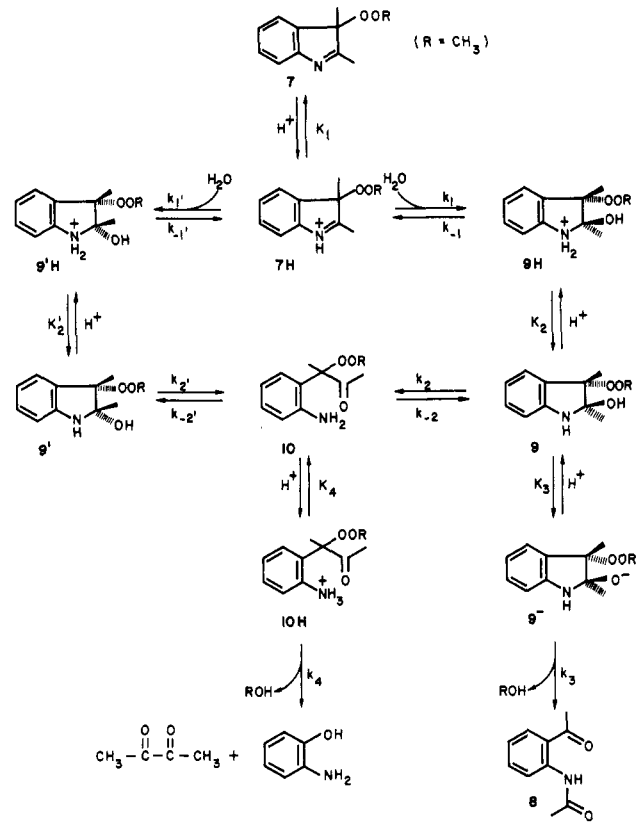

Discussion

All the results suggest that **6** and **7** react under the conditions of this investigation by a heterolytic mechanism. Such an interpretation agrees with literature data on related systems.[6-11,22] Specific indications that free-radical processes are not involved in the present reactions are the observations that O_2 has no effect on the reaction and that the rate in neutral ethanol is less than 2% of that in water at pH 7.

Mechanisms for the Reaction of 7. The effect of pH on the rate of the reaction of **7** and on the product distribution (Figure 1) is somewhat surprising because a bell-shaped curve is seen for the formation of each product. Since **7** undergoes only one ionization (pK_a = 2.2) over the pH range from 1 to 9, the observation of bell-shaped curves indicates that neither product is formed by a one-step reaction of **7** (or its protonated form); there must be at least one intermediate along the pathway to each of the two products. Only by the ionization of an intermediate or by a change in the rate-determining step can one explain the presence of the bell-shaped curves. Another general point concerning the data of Figure 1 is that, although k_{biac} decreases and k_{amide} increases around pH 6, one cannot explain the changes simply by competition for a single intermediate because k_{biac} decreases more than k_{amide} increases. This suggests that there must be some pathway to biacetyl in addition to one that can lead to either biacetyl or **8**.

The simplest mechanism that we have found which is consistent with all the data is that shown in Scheme I. Key intermediates in this mechanism are hydrates of **7** that can exist in *trans*-**9** and *cis*-**9′** forms as well as in protonated and unprotonated states (only one form of kinetically equivalent structures is shown in the scheme; enantiomers of **9** and **9′** will also be present). This mechanism qualitatively fits the experimental data in the following ways. At high pHs (7.5–9.0) where k_{obsd} increases with increasing $[H^+]$, the rate-determining step is presumably the formation of **9H** and **9′H** by attack of water on **7H**, which will be present at low (pK_1 = 2.2) but increasing concentrations as $[H^+]$ increases. Under these conditions **8** is the product because the K_3k_3 path is favored by high pH while the K_4k_4 path to biacetyl is not. As the pH is lowered, the K_3k_3 path to **8** becomes less favorable (pK_3 = ca. 14)[23] while that to biacetyl will be increasing (pK_4 = ca. 4). Around pH 4–5 the k_2 and $k_{2'}$ steps become rate limiting, and when **9** and **9′** become protonated (pK_2 = ca. 3.5)[23] at low pH, then the rate drops off. Several steps in the proposed mechanism are analogous in many of their features to mechanisms that have been suggested for the hydrolysis of imines.[24,25] It is clear from such studies that water attacks only the protonated form of the imine, as we suggest, and that amine expulsion (k_2 and $k_{2'}$ steps) occurs from a neutral, but presumably zwitterionic, form of the intermediate carbinolamine. Furthermore, such steps are usually not subject to general acid and base catalysis, and that is consistent with our observation of no buffer catalysis in the present reaction.

Extensive efforts were made[21] to fit the data to less complex mechanisms, but none were adequate. A key feature of the proposed mechanism is that only one of the geometric isomers of the carbinolamine intermediate can react at an appreciable rate to give **8**, but both can give biacetyl through the ring-opened structure **10**. In Scheme I, the trans isomer is shown as the species that can react to give **8**, but all the data would be equally consistent with its being the cis isomer rather than the trans. For mechanistic reasons (see later), it seems more likely that the trans would give **8** more rapidly. If one attempts to fit the kinetic and product data to a mechanistic scheme in which both the cis and trans isomers can react equally well to give **8**, then one finds that the calculated k_{obsd} in the pH 6–7 region is always 2- to 3-fold higher than what is observed. The data also cannot be fit to a scheme in which biacetyl is formed only from one geometric isomer of the carbinolamine and **8** from the other. In considering specific pathways to biacetyl, we had to eliminate the possibility that **9** or **9′** could react to give biacetyl directly without **10** and **10H** as intermediates, because such a mechanism predicts that biacetyl should be formed to higher pHs, i.e., until the k_1 and $k_{1'}$ steps become limiting. Similarly, **9** cannot react directly to give **8** without the prior deprotonation to **9⁻** because such a mechanism predicts that **8** should be formed down to lower pHs (3–4) where the k_2 and $k_{2'}$ steps are rate limiting for biacetyl formation.

The above qualitative discussion suggests that the experimental data can be fit by the mechanism of Scheme I, but this can be shown quantitatively as well. Using the steady-state assumption, one can derive the expression shown in eq 5, which relates the

$$k_{obsd} = \{(k_1bc' + k_{1'}bc)[H^+]^2 + (k_1b + k_{1'}b + k_1abc')[H^+] + (k_{1'}ab + k_1ac' + k_{1'}ac + k_1ab)(k_1 + k_{1'})a/[H^+]\}/\{(K_1 + [H^+])[bcc'[H^+]^2 + (bc' + cc' + bc + c^2k_{1'}/k_1) \times [H^+] + (abc' + b + c + ck_{1'}/k_1) + (c' + b + ck_{1'}/k_1)a/[H^+] + a/[H^+]^2]\} \quad (5)$$

$$a = \frac{k_3K_3}{k_2} \qquad b = \frac{k_4}{k_{-2}K_4} \qquad c = \frac{k_{-1}}{k_2K_2} \qquad c' = \frac{k_{-1'}}{k_{2'}K_{2'}}$$

constants of Scheme I to $[H^+]$ and the observed first-order rate constant. Similarly, the expressions for k_{amide} and k_{biac} can be derived, and these are given in eq 6 and 7, respectively. In order

$$k_{amide} = (k_1abc'[H^+] + (k_1ac' + k_{1'}ac + k_1ab) + (k_1 + k_{1'})a/[H^+])/(\text{same denominator as in eq 5}) \quad (6)$$

$$k_{biac} = ((k_1bc' + k_{1'}bc)[H^+]^2 + (k_1b + k_{1'}b) \times [H^+] + k_{1'}ab)/(\text{same denominator as in eq 5}) \quad (7)$$

to obtain values for the various constants in these relatively formidable equations, one general assumption is made, namely, that $c = c'$. This is probably a fairly good assumption because K_2 should be approximately the same as $K_{2'}$, and although k_{-1} may

(22) Witkop, B.; Patrick, J. B. *J. Am. Chem. Soc.* **1951**, *73*, 2196–2200.

(23) Fox, J. P.; Jencks, W. P. *J. Am. Chem. Soc.* **1974**, *96*, 1436–1449.

(24) Schmir, G. L. *J. Am. Chem. Soc.* **1965**, *87*, 2743–2751.

(25) Jencks, W. P. "Catalysis in Chemistry and Enzymology"; McGraw-Hill: New York, 1969; Chapter 10.

not equal $k_{-1'}$, any difference in these values should be reflected in similar differences in k_2 and $k_{2'}$. Assuming that $c = c'$, then at low pH (4 and below), where the $[H^+]^2$ terms dominate, eq 5 and 7 simplify to eq 8. By use of the expermentally determined

$$k_{obsd}(K_1 + [H^+]) = \frac{k_1 + k_{1'}}{c} \quad (8)$$

value for K_1 (6.6×10^{-3}), it was found that the data do follow such a relation in this pH region, and a value of 3.0×10^{-6} M s^{-1} for $(k_1 + k_{1'})/c$ is thus obtained. At very high pH, eq 5 and 6 should ultimately simplify to eq 9, from which a value for k_1

$$k_{obsd}K_1/[H^+] = k_1 + k_{1'} \quad (9)$$

$+ k_{1'}$ should be obtainable. Although it is not clear whether data were taken at a high enough pH for this to hold exactly, extrapolation of the values obtained with data points from pH 7.5–8.5 suggests that $k_1 + k_{1'}$ is ca. 100 s^{-1}. It turns out that the fit of the data is not too dependent on the specific value chosen, but the best fits[21] are obtained when $k_1 + k_{1'}$ is between 75 and 130 s^{-1}. In contrast to the limited flexibility in choosing a value for $k_1 + k_{1'}$, it was found by trial and error methods that the specific value chosen for k_1 is very important; one can only correlate the data at pH 6.5–7 if k_1 is 20 ± 2 s^{-1}. Further considerations indicated that the value calculated for k_{obsd} at pH 6 is very dependent on the c/b ratio; only when this is ca. 7 can adequate agreement with the experimental data be obtained. Finally, the k_{amide}/k_{biac} ratio is dominated by a/b, and adequate correlations of these data in the pH region 5.5–6.5 could only be achieved when a/b is ca. 3.7×10^{-13} M^2. Thus, when specific values for k_1 and for $k_1 + k_{1'}$ are chosen, there is very little flexibility possible in the values that can be used for the other constants of eq 5–7. The lines illustrated in Figure 1 were calculated by using the following specific values for the constants: $k_1 = 18.9$ s^{-1}, $k_1 + k_{1'} = 94.5$ s^{-1}, $a = 1.72 \times 10^{-6}$ M, $b = 4.63 \times 10^6$ M^{-1}, and $c = c' = 3.15 \times 10^7$ M^{-1}. It can be seen that the data are correlated reasonably well by these calculated lines, and therefore, the mechanism of Scheme I is consistent with the experimental results. Using estimated values[23] for $pK_2 = 3.5$, $pK_3 = 14$, and $pK_4 = 4$, one can calculate from a, b, and c the following approximate ratios: $k_3/k_2 = 2 \times 10^8$, $k_4/k_2 = 5 \times 10^2$, and $k_{-1}/k_2 = k_{-1'}/k_{2'} = 1 \times 10^4$. The fact that all of these ratios seem quite reasonable is a further indication that the reaction could proceed by the mechanism of Scheme I.

The detailed mechanism by which $\mathbf{9}^-$ is converted to **8** is of particular importance to this work. The finding that no ^{18}O from the peroxide ends up in the amide carbonyl is consistent with either the linear mechanism (pathway a of the introduction) or the Criegee rearrangement mechanism (eq 10) involving $\mathbf{9}^-$ rather

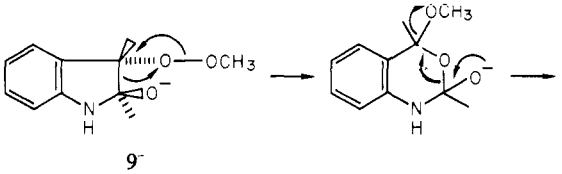

$\mathbf{9}^-$

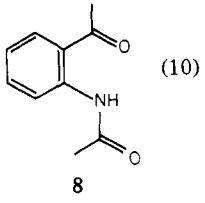

8 (10)

than the α-imino peroxide that was illustrated in eq 1. Since carbon to oxygen migrations involve a partial buildup of positive charge on the migrating group, the adjacent alkoxide would be expected to stabilize the transition state of the rearrangement mechanism. However, it is difficult to understand why only one geometric isomer of **9** can react if this is the mechanism. On the other hand, if the reaction proceeds by the linear mechanism, then one can at least rationalize this result because analogous reactions appear to require a trans antiparallel relationship of reacting groups.[26,27] For this reason the linear mechanism is favored for the present reaction.

It seems certain that biacetyl arises by a mechanism that involves a 1,2 carbon to oxygen migration of the aryl group. Usually such reactions require strong acid catalysis, but a structure kinetically equivalent to **10H**, i.e., one with a proton transferred from the amino to the methoxy group, might be expected to rearrange readily because the leaving group would be neutral methanol and the amino function could stabilize the partial positive charge developed on the migrating group in the transition state.

Mechanisms for the Reaction of 6. All the reaction steps and intermediates required to correlate the data obtained with **7** are also expected with **6**, but it is clear from a comparison of Figures 1 and 2 that other steps and intermediates are involved as well. Thus, the greater complexity of the reaction of **6** makes it impossible to fit the data quantitatively in any meaningful way. Nevertheless, one can come to some mechanistic conclusions from a qualitative analysis of the results, especially when they are considered in conjunction with the more detailed conclusions derived from the investigation of **7**.

Both the absolute values of k_{biac} and $k_{^{16}O\text{-amide}}$ from pH 3 to 6 or 7 and their changes with pH are very similar to those observed when **7** is reacted. Therefore, in this pH region presumably the main mechanisms for the formation of these respective products from **6** are the same as those found for **7**. In addition to these pathways, with **6** as the reactant there must be *at least* three other pathways to products, namely, (a) a pathway to biacetyl at low pHs (0–3), (b) a pathway to ^{18}O amide from pH 1–12.6, and (c) an additional pathway to ^{16}O amide at high pHs (7–12.6). One reaction possible with **6** and not with its methylperoxy analogue is the formation of a dioxetane (**11**), and it seems likely that this is an important intermediate, not only in the formation of some of the ^{18}O amide, but also in the formation of biacetyl at pH 0–3. Possibilities consistent with the data are outlined in Scheme II. If **11** is formed from neutral **6** (probably the zwitterionic form) and reacts directly to give **8**, then the decrease in the rate constant for formation of **8** at low pH can be attributed to the protonation of **6** ($pK_a = 2.28$). If biacetyl arises from a protonated form of **11**, then one can explain the general shape of the k_{biac} vs. pH curve (Figure 2) from pH 0 to 3 if the **6** to **11** conversion is a rapid equilibrium at pHs above 1 but becomes rate determining at low pHs where **6** is mainly present as **6H**. One can envisage several minor variations on the mechanism of Scheme II (for example, involving a perepoxide intermediate), but, in general, mechanisms of this type, in addition to those found for **7** (Scheme I), can adequately account for the data of Figure 2 from pH 0 to ca. 6.

The only reasonable mechanism by which ^{16}O amide can be formed from the reaction of **6**-^{18}O in $H_2{}^{16}O$ is if **6** initially hydrates to the carbinolamine and this intermediate decomposes by some mechanism to **8**. However, a problem arises when the reactions of **6** are compared with those of **7** because it was concluded that the formation of the carbinolamine becomes rate determining in the pH 7–8 region when **7** is the reactant, whereas the results in Figure 2 indicate that ^{16}O amide is formed up to pH 12 or more. A possible rationale for this finding is that the zwitterionic form of **6** hydrates more readily than **7** (which cannot give a zwitterion), possibly by an intramolecular general base catalyzed reaction as shown in Scheme III. For steric reasons, this is expected to result in the cis carbinolamine (**12**) being formed which previous indications suggest does not break down readily by the linear mechanism to **8**. However, with **6** as the reactant, this intermediate can ionize to the peroxy anion **15**, and recent evidence[11] suggests that peroxy anions undergo the Criegee rearrangement mechanism very readily. If this occurred with $\mathbf{12}^-$, then $\mathbf{13}^-$ would be formed. It is expected that $\mathbf{13}^-$ would decompose readily to **8**, but the detailed mechanism by which it does this will determine how much ^{18}O (in Scheme III the oxygens that would have ^{18}O

(26) Banthorpe, D. V. "Elimination Reactions"; Elsevier: New York, 1963; p 105.
(27) Sanchez, A. G.; Toledano, E.; Guillen, M. G. *J. Chem. Soc., Perkin Trans. 1* **1974**, 1237–1243.

Scheme II

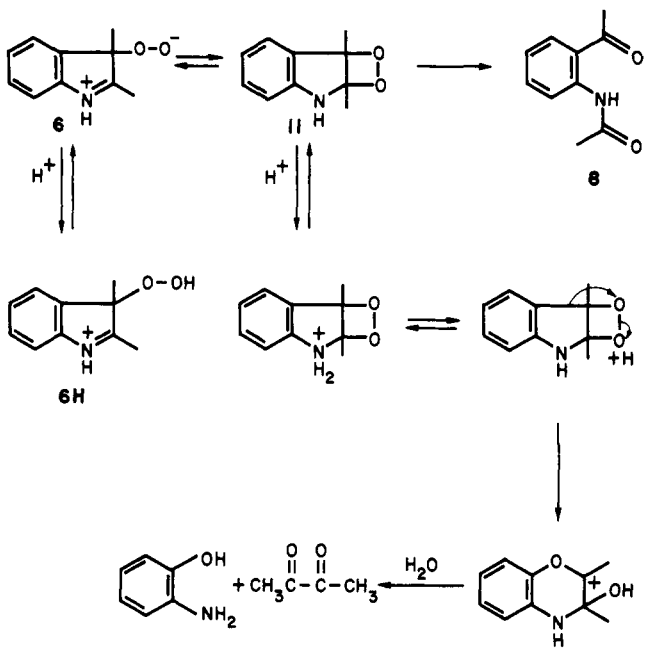

Scheme III

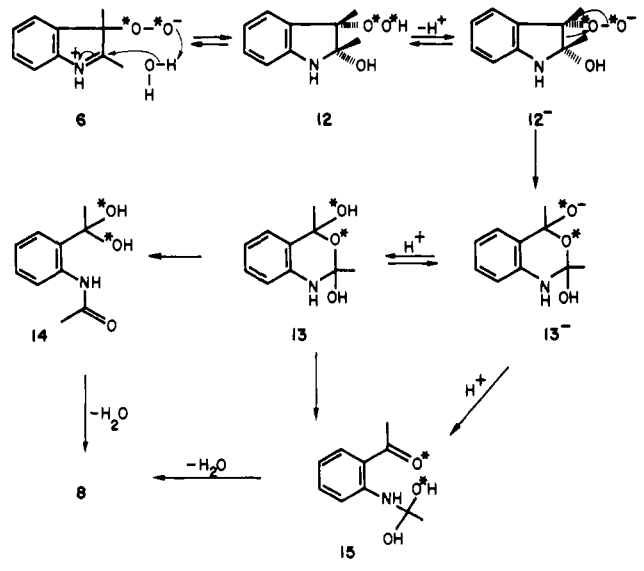

if 6-^{18}O is the reactant are indicated by asterisks) will end up in the amide carbonyl of **8**. If it decomposes by intermediate **14**, then no ^{18}O will be in the amide of **8**, while 50% ^{18}O in this position is expected if the decomposition occurs with **15** as an intermediate. It is of some interest that almost exactly 50% of the amide is labeled with ^{18}O from pH 9 to 12.6 (Figure 2 and Table II). Whether this is due to a mechanism involving **15** or is the result of two mechanisms competing equally, one giving only ^{18}O amide (for example, the dioxetane mechanism) and another giving only ^{16}O amide, is not clear at this time. However, the data in Figure 2 taken in conjunction with that found for **7** do indicate that there must be at least two mechanisms to give ^{16}O amide, and some kind of rearrangement mechanism such as outlined in Scheme III seems like a reasonable possibility. Since carbon to oxygen migrations occur more readily when the migrating group can stabilize a positive charge, one can understand why the carbinolamine would rearrange more readily than the reactant.

Possible Relevance to the Enzymic Reactions. Perhaps the most surprising result of the present investigation is that there are so many mechanisms that seem to be competing with one another under conditions that are very close to physiological. With **6** as the reactant at 41 °C and pH 5–10, the three general mechanisms originally considered for forming the amide, namely the linear mechanism, the dioxetane mechanism, and a rearrangement mechanism, all seem to be occurring. Therefore, it would not be surprising if examples of all three types of mechanisms will be observed in various enzymic reactions.

Recent evidence indicates that enzymes that catalyze the cleavage of phenols proceed by a rearrangement mechanism,[12,13] and it seems likely that this mechanism may be involved in most dioxygenase reactions.[5] The present results suggest that one way an enzyme could catalyze such a reaction would be to have some nucleophilic group (most probably an oxygen or nitrogen nucleophile) on the enzyme function like the water does in the mechanism of Scheme III. This mechanism is entirely consistent with the observation that such reactions proceed to give products with both atoms of oxygen coming from O_2 because, with an enzymic group in the position of the unasterisked OH, the only way an intermediate analogous to **13** could give product is to split out the enzymic group, thus giving the product with two labeled oxygens. It will be interesting to see whether some nucleophilic group on these enzymes does function in this capacity.

Experimental Section

Materials. Unless otherwise noted, all commercially available materials were of analytical or reagent grade and were used without further purification. ^{18}O-enriched H_2O (20.0 and 10.0 atom % ^{18}O) was obtained from Bio-Rad and 99.7% D_2O from Aldrich. $^{18}O_2$ was prepared by electrolysis of $H_2{}^{18}O$ (20.0 atom % ^{18}O). 2,3-Dimethylindole (Aldrich, 99%) was purified by sublimation immediately prior to use. The sublimate was a perfectly white solid of sharp melting point (mp 107–108 °C), which gave only one spot on TLC analysis (R_f 0.60, 9:1 benzene–ether as solvent). 2,3-Butanedione (biacetyl, Aldrich practical grade) was purified by distillation and that fraction boiling at 86 °C collected. The purified material showed no extraneous peaks by GC analysis. *o*-Acetamidoacetophenone (**8**) was prepared as described by Leonard and Boyd,[28] and 2,3-dimethyl-3-(hydroperoxy)indolenine (**6**) by the method of Berti et al.[29] The latter material, which was stored at −6 °C, had the following characteristics: mp 102–104 °C dec; NMR ($CDCl_3$) δ 1.42 (s, 3 H, 3-methyl group), 2.14 (s, 3 H, 2-methyl group), 7.25 (m, 4 H, aromatic protons), and about 13 (br s, 1 H, OOH); IR (KBr) 3050, 2600, 1600, 1430, 760 cm^{-1}; UV λ_{max} (EtOH) nm (ϵ) 260 (3300), 280 (2700), λ_{min} 235 (1880); TLC, only one spot seen in 9:1 benzene–ether, R_f 0.11 (KI active), and in 20:3 toluene–methanol, 0.43 (KI active). ^{18}O-enriched **6** (**6**-^{18}O) was prepared by the same method[30] with $^{18}O_2$ as the reactant; special precautions[21] were taken to avoid contamination by O_2.

2,3-Dimethyl-3-(methylperoxy)indolenine (7). A solution of 400 mg (2.3 mmol) of **6**, 0.2 mL (2.1 mmol) of dimethylsulfate, and 2 mL of 1 M (2.0 mmol) NaOH in 50 mL of ethanol was stirred at room temperature for 1 h and then cooled to 0 °C. All subsequent purification steps were performed at 0 °C, and those in which the product was in contact with aqueous media were carried out as rapidly as possible. After evaporation of the ethanol, the residue was swirled with 25 mL of anhydrous ether, and the resulting ether solution was washed first with 2 M KOH (two 10-mL portions) to remove unreacted **6**, then washed with 10 mL of 0.1 M succinate buffer (pH 5.0), and finally extracted with 1.24 M HCl (two 10-mL portions). The acid extracts were immediately neutralized by draining into 10 mL of water containing 4 g of sodium acetate (a 2-fold excess over the amount of HCl). At this point **7** separates as a pale yellow oil. The heterogeneous mixture was extracted with 25 mL of ether, and the ether layer was dried over $MgSO_4$, filtered, and stored at −6 °C as a stock solution. TLC analysis (9:1 benzene–ether) of this material showed only one KI active spot with an R_f of 0.36. Material purified by TLC had the following UV: λ_{max} (EtOH) nm (ϵ) 240 (2400), 260 (3190), and 280 (2380). On the basis of UV analysis of the stock solution, the yield of **7** is 50%. For NMR analysis the ether was removed from the stock solution by evaporation and pumping under vacuum. The spectrum of the pale yellow liquid taken immediately in $CDCl_3$ is as follows: δ 1.40 (s, 3.2 H, 3-methyl), 2.31 (s, 2.9 H, 2-methyl), 3.62 (s, 3.0 H, *O*-methyl), and 7.33 (m, 4 H, aromatic protons). The NMR spectrum also shows the presence of acetic acid (δ 2.05 and 11) in about the same concentration as **7**, but otherwise no peak was seen whose area is greater than 1% that of the methyl groups. Less than 3% of **6** is present, as indicated by TLC analysis. Ether stock solutions of

(28) Leonard, N. J.; Boyd, S. N., Jr. *J. Org. Chem.* **1946**, *11*, 405–418.
(29) Berti, G.; Da Settimo, A.; DiColo, G.; Nannipieri, E. *J. Chem. Soc. C* **1969**, 2703–2710.
(30) Albert, A.; Sargeant, E. P. "Ionization Constants of Acids and Bases"; Wiley: New York, 1962; pp 69–91.

7 were not indefinitely stable because some yellowing occurred with time. Solutions were only used as long as the UV spectrum was within 10% of freshly prepared solutions, only one KI active spot was seen on TLC, and the yield of products obtained on reaction in aqueous solution was greater than 85%.

2,3-Dimethyl-3-(methylperoxy)indolenine with ^{18}O in the peroxide oxygens (**7**-^{18}O) was prepared by a procedure similar to that described above. TLC analysis indicated that the preparation of **7**-^{18}O had only one KI-active spot, but it was contaminated with a small amount of **8** (R_f 0.42 with 9:1 benzene–ether. The ^{18}O content of **7**-^{18}O was assumed to be the same as that of the **6**-^{18}O from which it was prepared.

General Analytical Methods. Nuclear magnetic resonance (NMR) spectra were obtained with a Varian Model A-60A spectrometer, infrared (IR) on a Perkin-Elmer Model 735, ultraviolet–visible (UV–vis) on either a Cary Model 14 or Cary Model 118 recording spectrophotometer, mass spectra (MS) on an Associated Electronic Industries MS-902, and GC–MS on a Finnegan Model 3200 GC–MS equipped with a 5-ft Chromasorb 101 column. Gas chromatographic work (GC) was conducted on a Perkin-Elmer Model 880 gas chromatograph equipped with a dual flame ionization detector and dual columns (4-ft Carbowax 20M, 5% on Chromasorb Z or 10-ft Chromasorb 101). Nitrogen was used as the carrier gas. Columns were conditioned overnight at a temperature 50 °C below that at which they were to be used and subsequently for a few hours at the appropriate temperature. Kinetic experiments were monitored with a Gilford Model 240 UV–vis spectrophotometer equipped with a Gilford Model 6040 strip chart recorder, an automatic sample changer, and a constant temperature accessory. Thin layer chromatography (TLC) was done with silica gel plates (Eastman Chromagram Sheet No. 13181) containing fluorescent indicator. Spots were visualized under UV (254 nm) irradiation and sprayed, when necessary, with 1% aqueous potassium iodide solution. All pHs were measured at the same temperature as the kinetic runs.

Kinetic Methods. Unless otherwise indicated, kinetic experiments were performed at 41 ± 0.1 °C, each reaction mixture contained 0.1 mM EDTA, and the ionic strength was kept constant at 0.30 by adding KCl in addition to the buffer. Three concentrations of buffer (0.01, 0.05, and 0.10 M usually) were used at each pH, and at least two kinetic runs were done at each of the buffer concentrations. In those ranges of pHs in which it was necessary to change from one buffer to another, the different buffers were both employed at the same pH in order to ensure that the identity of the buffer had no effect on the course of the reaction. Runs were initiated either by direct addition of aliquots (0.02–0.05 mL) of a cold ether stock solution of **6** or **7** or by addition of an aliquot (0.1 mL) of a freshly prepared stock solution in cold H_2O–*tert*-butyl alcohol (made by dissolving about 2 mg in 0.4 mL of *tert*-butyl alcohol and diluting to the appropriate volume with chilled water) to 3.0 mL of buffer. The reaction mixtures thus contained H_2O (98.4)–Et_2O (1.6) and H_2O (99.4)–*tert*-butyl alcohol (0.6), respectively. The temperature of the resulting solution was thereby lowered slightly (<1 °C). This was seen in the first-order kinetic plots as a slight induction period in the very early stages of the reaction, but the k_{obsd} value was not affected significantly. The range of concentrations of reactant employed was 0.1–1 mM. At pH 5.0 and below, the reaction was followed at either 260 or 280 nm, at which wavelengths the absorbance value decreases with time while at higher pHs the absorbance increase with time was monitored at 325 nm. First-order kinetic plots of the data were usually linear over the time period corresponding to 2–3 half-lives, and the reproducibility of the derived rate constants was ±5% of their value. The value of the first-order rate constant (k_{obsd}) was calculated from the slope of a plot of log ($\lambda_\infty - \lambda_t$) vs. t (λ_∞ is the absorbance after 8–10 half-times) when an increase in absorbance at a particular wavelength was followed, and of a plot log ($\lambda_t - \lambda_l$) vs. t otherwise. Complete UV spectra were routinely taken for each run at the completion of the reaction.

Determination of the pK_as of Protonated 6 and 7. The UV spectra of **6** and **7** in their protonated and neutral forms are sufficiently different to allow determination of their pK_as by spectral measurements according to a general method given by Albert and Sergeant.[30] Maximum differences in absorbance occurred around 250 and 300 nm so these wavelengths were used for the pK_a determinations. Preliminary results suggested an approximate pK_a of 2.3, so a series of 0.1 M chloroacetate buffers covering the pH range 1.7–2.9 in 0.2 pH unit steps were prepared and thermostated at 41.0 °C, and the absorbance of **6** or **7** (0.2 mM) in each of these, as well as under conditions in which they exist entirely in one form (i.e., completely protonated in 1.24 M HCl; completely unprotonated at pH 5.0), was recorded. Absorbances were measured as a function of time and extrapolated to give a value for zero time. The pK_a was calculated from the data by eq 11, where A_m, A_i, and A are the

$$pK_a = pH + \log (A - A_m)/(A_i - A) \quad (11)$$

respective zero-time absorbances of the fully unprotonated, fully protonated, and the partially protonated **6** or **7** at that particular pH.

Identification of 2,3-Butanedione (Biacetyl) as a Product by GC–MS. A reaction mixture (50 mL) containing 3 mM **7** and 0.1 M chloroacetate buffer (pH 1.9) was allowed to react at 40 °C for 12 h (ca. 5.5 half-lives), following which it was extracted with three 20-mL portions of ether. After concentration by evaporation of most of the ether, the material was subjected to GC–MS analysis.

Analytical Gas Chromatography. Biacetyl was analyzed with a 10-ft Chromasorb 101 column operating isothermally at 140 °C (injector temperature, 160 °C). Either *n*-butyl alcohol or 2-nitropropane was used as an internal standard for these analyses. Following addition of the internal standard to completed reaction mixtures and extensive shaking, a small aliquot (3 μL) of the solution was injected directly into the GC. The amount of biacetyl was then calculated from the peak heights corresponding to biacetyl and the internal standard compared to the heights obtained when aliquots of control solutions are injected. In the controls, weighed amounts of biacetyl and the internal standard were added to solutions that had everything identical with the reaction mixtures except they did not contain any **6** or **7**. Results of duplicated analyses were usually reproducible to within ±5%.

o-Acetamidoacetophenone (**8**) was analyzed on a 4-ft Carbowax 20M (5% on Chromasorb Z) column operating isothermally at 188 °C (injector temperature, 200 °C). *p*-Cyanoacetophenone was used as the internal standard. Following addition of the internal standard and 0.1 mL of 1,2-dichloroethane to 3-mL reaction solutions and shaking for 10 min, a 1-μL aliquot of the dichloroethane layer was injected into the GC. The calculation of the amount of **8** present was done as described above for biacetyl. Again the controls that had weighed amounts of **8** and the internal standard were treated in the same way as the reaction mixtures. Multiple analyses were generally reproducible to ±5%.

Reactions of ^{18}O-Labeled 6 and 7. In a typical run, 5 mg of **6**-^{18}O (or **7**-^{18}O) dissolved in 0.2 mL of *tert*-butyl alcohol was added to 10 mL of buffer, and the reaction was allowed to proceed at 40 °C for approximately 10 half-lives. For analysis of the product with the AEI MS-902 mass spectrometer, the reaction solutions were cooled to room temperature and extracted 3 times with 3-mL portions of 1,2-dichloroethane; the extracts were pooled, evaporated to dryness, and further dried overnight in a vacuum desiccator, and the residue was injected directly into the mass spectrometer. For analysis with the GC–MS technique, benzene was used as the extraction solvent, and the extracts wre concentrated to ca. 1 mg of product per mL prior to injection onto the column.

At high pHs (12.5 and above), base-catalyzed exchange of the amide oxygen becomes a significant factor and necessitated an alteration in the procedure. To 25 mL of thermostated buffer was added a solution of 24.9 mg of **6**-^{18}O in 0.4 mL of 1,4-dioxane, and aliquots (5 mL) of the reaction mixture were withdrawn at specified times, cooled to 0 °C, and extracted with benzene (two 5-mL portions). Unreacted **6**-^{18}O was removed from the pooled benzene extracts by extraction with cold 2 M KOH (10 mL), and then immediately the benzene layer was washed with saturated NaCl solution (10 mL) and neutralized by washing with pH 6.0 succinate buffer (three 10-mL portions). The benzene was removed by rotary evaporation and the residue dried overnight in a vacuum desiccator before being subjected to mass spectral analysis. For reactions of **6**-^{18}O in ethanolic sodium ethoxide, the product was isolated by first removing the ethanol by evaporation, followed by swirling with water and extraction with benzene as described above.

Mass Spectrometry. The ^{18}O enrichment of **6**-^{18}O was determined from the relative intensities of the ions at m/z 179 and 177. These relative intensities were obtained at 70 eV on an AEI MS-902 mass spectrometer, with the data being presented as a series of low-resolution digital plots of that portion of the mass spectrum of **6**-^{18}O around m/z 177 (the m/z for the molecular ion). The ratios of the intensity at m/z 179 to that at m/z 177, hereafter represented symbolically as $I_{179/177}$, for each low-resolution digital plot (5–8 usually obtained during an analysis) were averaged to give the value used in the calculations. Since **6** is thermally unstable at temperatures similar to those employed in this analysis (about 180 °C), the observed mass spectrum is probably due to decomposition products of **6**. The portion of the mass spectrum in the region around m/z 177 is, however, well separated from other ions (i.e., no ions are present having an m/z higher than 177 other than those due to isotopic substitution and no ions are present of significant intensity in the m/z region from 176 to 167) in the spectrum and is probably due to an ion having the same formula as **6** (possibly **8**).

The position and extent of ^{18}O labeling of **8** were determined from measurements of the $I_{179/177}$ and $I_{137/135}$ ratios. These ratios were routinely obtained from a low-resolution digital plot of the mass spectrum of **8**, and the reported values are averages of at least five such plots. In addition, some samples of **8** were analyzed by GC–MS on a Finnegan 3000 D GC–MS (equipped with a 5-ft Carbowax 20M, 5% on Chromasorb Z column). Mass spectra were taken rapidly (every 2 s) before,

during, and after elution of the peak due to **8**, and the sum of the intensities of the ion of m/z 179 was related to that of the ion of m/z 177. The $I_{137/135}$ ratio was similarly obtained.

Calculations of Oxygen-18 Content. Unless otherwise noted, all intensity ratios reported are corrected for natural abundance contributions and are thus representative of isotopic enrichment of a particular isotope. These corrections were made in the case of **6** by subtracting from the experimentally observed $I_{179/177}$ the $I_{179/177}$ calculated for an ion of formula $C_{10}H_{11}NO_2$ from natural abundance levels of isotopes ($I_{179/177,calcd}$ = 0.010, from mass spectral tables). Although corrections to $I_{179/177}$ and $I_{137/135}$ could be made similarly in the case of **8**, the values subtracted from these observed ratios were experimentally obtained by analysis of standard unlabeled **8** analyzed immediately before analysis of labeled samples of **8**. Analysis of standard **8** was done in order to ensure that the MS technique was accurate from day to day.

For a compound containing two atoms of a particular element (in this case, oxygen), the isotopes of which are randomly distributed between the two positions and in which a = relative amount of the oxygen that is ^{16}O and b = relative amount that is ^{18}O, then eq 12 gives the relative

$$(a + b)^2 = 1 = a^2 + 2ab + b^2 \quad (12)$$

distribution of the various isotopic species.[31] Thus, for **6** and **8**, whose molecular weights are both 177, $2ab/a^2 = I_{179/177}$. Since $b = 1 - a$, then both a and b can be obtained from the $I_{179/177}$ ratio. In the particular preparation of **6**-^{18}O used for most of the work reported, the values of a and b were 0.843 and 0.157, respectively. Therefore, the relative intensities of the various labeled species were as follows: **6**-$^{18}O,^{18}O = b^2$ = 0.025, **6**-$^{16}O,^{18}O = 2ab$ = 0.265, and **6**-$^{16}O,^{16}O = a^2$ = 0.710.

o-Acetamidoacetophenone (**8**) contains two chemically different oxygens, a nonexchangeable amide oxygen and a readily exchangeable ketone oxygen. As indicated in the Results section, the ion of m/z 135 results from loss of ketene from the amide portion of **8**. Measurement of the labeling extent in this fragment ion, which now contains only one oxygen, the ketone oxygen, may be used to obtain not only the amount of labeling at this position but, by difference, the amount of labeling of the amide oxygen.

(31) Biemann, K. "Mass Spectrometry: Organic Chemical Applications"; McGraw-Hill: New York, 1962; p 65.

The fraction of the ketone oxygen that has undergone exchange (KE) with solvent oxygen may be obtained from eq 13, where $I_{137/135,calcd}$ is the

$$KE = 1 - (I_{137/135}/I_{137/135,calcd}) \quad (13)$$

expected ratio for an ion of formula C_8H_9NO containing relative amounts of ^{18}O to ^{16}O of 0.157:0.843. Knowledge of the fraction of the ketone oxygen of **8** that has undergone exchange allows calculation of a theoretical $I_{179/177}$ ratio (eq 14), which represents the expected result if all

$$I_{179/177,theor} = \frac{[(0.265/2) + (0.265/2)(1 - KE) + 0.025(KE)]}{0.710 + (0.265/2)(KE)} \quad (14)$$

of the amide oxygen originated from a peroxide oxygen of **6**. The percent of amide oxygen that actually becomes labeled with ^{18}O during the reaction may then be calculated by eq 15. Equation 14 includes terms

$$\% \text{ amide oxygen labeled} = \frac{(100)(I_{179/177} - I_{137/135})}{(I_{179/177,theor} - I_{137/135})} \quad (15)$$

that deal with complications leading to changes in the theoretical $I_{179/177}$ ratio arising from exchange of the ketone oxygen. Of the **6** initially used, 2.5% is labeled with ^{18}O in both oxygens and, since its molecular weight is 181, should not contribute to the theoretically predicted $I_{179/177}$. Exchange of the ketone oxygen leads, however, to an ion with a molecular weight of 179 and therefore directly affects the observed and theoretically predicted $I_{179/177}$ values. Following similar reasoning further, it can be seen that **6** contains 26.5% of $^{16}O^{18}O$ material. Since the peroxide oxygens are considered to be randomly labeled with ^{18}O, 26.5/2% of this material is labeled in a peroxide oxygen theoretically destined to be the ketone oxygen of **8** (and, therefore, exchangeable), and 26.5/2% is destined for the nonexchangeable amide oxygen of **8**. Exchange does not affect the latter oxygen but does lead to a lowering of the predicted I_{179} and a corresponding increase in the predicted I_{177} value due to exchange of the ketone oxygen.

When **6**-^{18}O was reacted in D_2O, there was a small amount of exchange of deuterium into the methyl ketone group. Therefore, in these cases before the percents of ^{18}O labeling were calculated by the methods described above, small corrections were made[21] on the observed $I_{179/177}$ and $I_{137/135}$ ratios. The magnitude of these corrections was determined from the relative intensities of the 178 and 136 peaks.

Registry No. 6, 13177-23-6; **7**, 67152-54-9; **8**, 5234-26-4.

Transmission of Substituent Effects through the Silicon–Silicon Bond

Gene M. Dubowchik, David W. Gottschall, Michael J. Grossman, Robert L. Norton, and Claude H. Yoder*

Contribution from the Department of Chemistry, Franklin and Marshall College, Lancaster, Pennsylvania 17604. *Received August 17, 1981*

Abstract: The transmission of substituent effects through the Si–Si bond was measured by monitoring $^{13}C–^{1}H$ coupling constants and ^{1}H, ^{13}C, and ^{29}Si chemical shifts in substituted disilanes of the type $XSi(CH_3)_2Si(CH_3)_3$ (X = F, Cl, Br, CN, OC_2H_5, $N(CH_3)_2$, CH_3) and through the NCH_3 $^{13}C–^{1}H$ coupling constants and basicities of the series $XSi(CH_3)_2Si(CH_3)_2N(CH_3)_2$ (X = Cl, OC_2H_5, $N(CH_3)_2$, CH_3). Coupling constants and ^{1}H and ^{13}C chemical shifts correlated well with a variety of inductive parameters. Comparisons with the carbon analogues indicated that the C–C linkage transmits substituent effects about twice as effectively as the Si–Si bond. Indeed, the silicon–silicon bond in some systems behaves virtually as an insulator rather than conductor of substituent effects. This difference can be attributed to electrostatic field effects without recourse to (p–d)π, (d–d)π, or dative interactions.

Explorations of the ability of the carbon–carbon linkage to transmit the effect of substituents have served as keystones for our present understanding of electrical and spatial effects in organic chemistry. The unsurpassed ability of carbon to catenate and thereby provide the greatest number of systems amenable to such studies has led, however, to a dearth of information about the transmission of substituent effects through other catenated linkages. Because of its ability to catenate and the fact that it is isoelectronic in valence electrons with carbon, silicon provides an excellent opportunity to study the effects of increased size (and consequently longer substituent–reaction site distance), greater polarizability, and the presence of d orbitals which allow for (p–d)π, (p–d–d)π, etc. interactions. The present study is an attempt to evaluate the transmission of electrical effects through the Si–Si bond in disilanes through the monitoring of $^{13}C–^{1}H$ coupling constants and ^{13}C, ^{1}H, and ^{29}Si chemical shifts in the

0002-7863/82/1504-4211$01.25/0